Diagnosis of Multiple Sensor and Actuator Failures in Automotive Engines

Pau-Lo Hsu, *Member, IEEE,* Ken-Li Lin and Li-Cheng Shen

***Abstract*—Unlike cases where only a single failure occurs, fault detection and isolation of multiple sensor and actuator failures for engines are difficult to achieve because of the interactive effects of the failed components. If faults all appear either in sensors only or in actuators only, many existing residual generators which provide decoupled residual signals can be employed directly to obtain proper fault detection and isolation. However, when both sensor and actuator failures occur at the same time, their mutual effects on residuals make fault isolation particularly difficult. Under such circumstances, further decision logic is required. In this paper, we propose a hexadecimal decision table to relate all possible failure patterns to the residual code. The residual code is obtained through simple threshold testing of the residuals, which are the output of a general scheme of residual generators. The proposed diagnostic system incorporating the hexadecimal decision table has been successfully applied to automotive engine sensors and actuators in both simulation and experimental analyses. Enhancement of the present diagnostic performance by implementing an additional sensor is also described.**

I. Introduction

IN COMPLEX automatic control systems safety and reliability are crucial. These are especially important in safety-critical cases such as nuclear power plants, aircraft, space vehicles, and processes that involve the handling of dangerous chemicals. If any failure occurs in such systems, it may lead to serious economic loss or hazards to personnel. Consequently, there is a need for a monitoring scheme that performs the tasks of failure detection, isolation, and accommodation. Various diagnostic systems have been proposed and analyzed [1]–[5]. In these systems, failure detection and isolation (FDI) are generally achieved in two stages: 1) residual generation and 2) decision making. The first stage generates a set of failure-sensitive signals called the residuals; the second stage detects and isolates the failures according to the characteristics of the residuals.

With the increasing application of electronically controlled engines in the automotive industry, fault diagnosis in automotive systems has become an important research and development topic. Several approaches have been reported to successfully detect and isolate either sensor or actuator failures, i.e., single failure occurrences, in automotive engines [6]–[8]. In practice, however, multiple failures in sensors, actuators, or both sensors and actuators may exist, making available diagnostic methods fail. Thus, a more powerful diagnostic system designed to cope with multiple failures is required. To localize the multiple sensor and actuator failures uniquely as they occur in a dynamic system, one needs, in general, a bank of observers rather than a single observer. Fault detection schemes with multiple Kalman filters have been developed for identifying multiple failures [9]–[11]. Furthermore, the dedicated observer scheme (DOS) has been applied to fault detection for multiple fault occurrences by using a bank of Luenberger observers [12], [13], where each instrument of interest drives an observer to perform a complete state estimation. Two restrictions arise in this type of multiple observer-based FDI scheme. First, since each observer in the scheme is driven by only one instrument output, the states of the plant should be completely observable through each instrument, and this does not always hold in practice. The second limitation in the DOS is that only a single failure is admitted at a single instant; that is, multiple failures occurring simultaneously in both sensors and actuators are difficult to identify. Therefore, extensions of diagnostic observer design for residual structure enhancement and further decision logic are necessary.

In this paper, we first synthesize a set of residual generators to construct a general scheme for multiple fault diagnosis. When all failures occur either in sensors or in actuators, the well-decoupled output residuals can be used directly for fault isolation. However, when multiple failures occur simultaneously in both sensors and actuators, fault isolation cannot be achieved merely by checking the residual outputs directly because of the interactive effects of the failed components. Therefore, a powerful approach involving a hexadecimal decision table is proposed here for further decision making. Both simulation and experimental results show that the present diagnostic system can effectively identify multiple sensor and actuator failures in engine systems.

II. A General Scheme for Residual Generators

For multiple failure diagnosis, synthesis of a set of model-based residual generators is commonly employed. In this paper, all faults of the dynamic system that need to be monitored are first assumed to occur in the same sector, either sensors or actuators. Then, a hexadecimal decision table is proposed to identify simultaneous faults in both sensors and actuators.

Consider a minimal state-space realization of the discrete-time plant model given by the following equations

$$x(k+1) = A\,x(k) + B\,u(k) + E\,d(k) \tag{1}$$

Manuscript received March 8, 1993; revised April 28, 1994. This work was supported by the National Science Council, Republic of China under Contract NSC-80-E-SP-009-02E.

The authors are with the Institute of Control Engineering, National Chiao Tung University, Hsinchu, Taiwan 300 R.O.C.

IEEE Log Number 9413002.

$$y(k) = C\,x(k) + D\,u(k) + F\,d(k) \tag{2}$$

where $x(k) \in \mathbf{R}^n$ is the state vector, $u(k) \in \mathbf{R}^p$ is the input vector, $y(k) \in \mathbf{R}^m$ is the measurement output vector, and $d(k) \in \mathbf{R}^q$ is the fault vector to be detected. In general, $d(k)$ consists of faults which may occur in the actuators, the plant dynamics (components), or the sensors. System parameters A, B, C, D, E, and F are constant matrices with appropriate dimensions. The initial state $x(0)$ is assumed to be zero. Taking the z-transformation of (1)–(2) gives

$$y(z) = G_u(z)u(z) + G_d(z)d(z) \tag{3}$$

where

$$G_u(z) = C(zI - A)^{-1}B + D \tag{4}$$

$$G_d(z) = C(zI - A)^{-1}E + F. \tag{5}$$

A residual generator can be expressed in a general form as [5], [14]

$$r(z) = F(z)u(z) + H(z)y(z) \tag{6}$$

with the properties that for all $u(z)$,

$$\text{i)}\quad r_i(z) = 0 \qquad \text{if } d_i(z) = 0 \text{ and} \tag{7}$$

$$\text{ii)}\quad r_i(z) \neq 0 \qquad \text{if } d_i(z) \neq 0,\ i = 1, 2, \ldots, q \tag{8}$$

where $F(z)$ and $H(z)$ are stable and proper transfer matrices that are realizable in a real system. When no failure occurs, all the residuals are equal or close to zero. In the presence of the i-th failure signal, the i-th residual signal will become distinguishably nonzero. Therefore, the fault may be detected and isolated by observing the residuals. By substituting (3) into (6), we can rewrite the residual vector r as

$$r(z) = [F(z) + H(z)G_u(z)]\,u(z) + H(z)G_d(z)d(z). \tag{9}$$

To generate the residual vector r with the properties described in (7)–(8), $F(z)$ and $H(z)$ must satisfy the following conditions

$$\text{i)}\quad F(z) \text{ and } H(z) \text{ are both stable and proper, and}$$

$$\text{ii)}\quad F(z) + H(z)G_u(z) = 0. \tag{10}$$

Condition i) implies that the dynamic system of the residual generator is stable, so that its undesired initial states will approach zero. Condition ii) ensures that $r(z)$ will be independent of input $u(z)$. Moreover, the desired residual map between faults and residuals in the design for real applications may be specified as $M(z)$. Thus, the following condition may be also satisfied

$$H(z)G_d(z) = M(z). \tag{11}$$

where

$$M(z) = \begin{bmatrix} \frac{\tilde{b}_1(z)}{a_1(z)} & & 0 \\ & \ddots & \\ 0 & & \frac{\tilde{b}_q(z)}{a_q(z)} \end{bmatrix} \tag{12}$$

with $a_i(z)$, $\tilde{b}_i(z) \in \mathbf{R}[z]$ and $\mathbf{Z}[a_i] \in \mathbf{C}_-$, $i = 1, 2, \ldots, q$, where $\mathbf{R}[z]$ is the ring of polynomials in z with real coefficients and poles of $\mathbf{C}_-$ within the unit circle. Equation (11) indicates that the map $M(z)$, from $d(z)$ to $r(z)$, is decoupled in order to identify different faults [15], [16]. There are many published methods that can be adopted to obtain the residual signals; as reported in [5], different approaches selected according to the preference of researchers or for different purposes may lead to identical design results. For example, the $M(z)$ of a fault identification filter (FIDF) [17] can be selected so as to obtain moving average forms for $F(z)$ and $H(z)$ in deadbeat responses to yield the parity space equations.

When faults occur in both sensors and actuators, as shown in Fig. 1, $\bar{u}(k)$ and $\bar{y}(k)$ correspond to the actual input and output of the plant, respectively, and $u(k)$ and $y(k)$ represent the desired input and measured output. The actuator and sensor failures are represented by $a(k)$ and $s(k)$, respectively. Thus, we have the following equations

$$y(k) = \bar{y}(k) + s(k) \tag{13}$$

$$\bar{u}(k) = u(k) + a(k) \tag{14}$$

where $s(k)$ is a time-varying vector with element $s_i(k)$ representing the failure signal of the i-th sensor. Several failure modes of the i-th sensor can be modeled by choosing $s_i(k)$ properly. For instance, if the i-th sensor completely fails, producing zero output, then $s_i(k) = -\bar{y}_i(k)$; if there is a bias error b_i appearing in the i-th sensor, then $d_i(k) = b_i$. The actuator failures $a(k)$ can be modeled in the same way [18]. Note that $\bar{u}(k)$ and $\bar{y}(k)$ are "internal" variables which are inaccessible. Therefore, we need to further combine (13) and (14) with the nominal plant model so that the state equations are explicitly expressed by the external variables $u(k)$ and $y(k)$. Thus, we obtain

$$x(k+1) = A\,x(k) + B\,u(k) + B\,a(k) \tag{15}$$

$$y(k) = C\,x(k) + s(k) \tag{16}$$

where $a(k) \in \mathbf{R}^p$ is the actuator failure vector and $s(k) \in \mathbf{R}^m$ is the sensor failure vector. Also, we have

$$y(z) = G_u(z)u(z) + G_s(z)s(z) + G_a(z)a(z) \tag{17}$$

where

$$G_u(z) = C(zI - A)^{-1}B$$

$$G_a(z) = G_u(z)$$

$$G_s(z) = I_{m\times m}.$$

The corresponding terms with the subscripts "s" and "a" in the following equations are designed with respect to sensor and actuator failures, respectively. To detect and isolate multiple sensor and actuator failures, a general scheme is proposed here to generate a set of residuals for decision making. Note that for a diagnostic system, the number of sensors used to extract failure information is usually greater than the number of actuators. Therefore, only cases where $m \geq p$ are discussed in this paper. Different residual generators can be designed separately for sensors and actuators as described below.

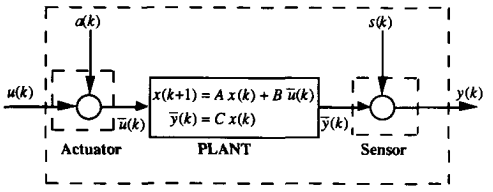

Fig. 1. Relationships between plant, sensor failures, and actuator failures.

A. Residual Generators for Sensor Failure Detection

To design residual generators specifically for sensor failure detection, we obtain $H_s(z)$ and $F_s(z)$ by choosing any desirable diagonal map $M_s(z)$ as follows

$$H_s(z) = M_s(z)G_s^{-1}(z) = M_s(z) \tag{18}$$

and

$$F_s(z) = -H_s(z)G_u(z) = -M_s(z)G_u(z). \tag{19}$$

Then, we have

$$\begin{aligned} r_s(z) &= H_s(z)y(z) + F_s(z)u(z) \\ &= M_s(z)(s(z) + G_u(z)a(z)). \end{aligned} \tag{20}$$

Equation (20) indicates that if only sensor faults occur, i.e., $a(z) = 0$, all multiple sensor failures can be detected by examining the residuals directly. However, when sensor and actuator fail simultaneously, both the sensor failure and actuator failure will contribute to the residual outputs specifically designed for sensors, as shown in (20). Thus, further decision making is required for the signals from these residual generators.

B. Residual Generators for Actuator Failure Detection

In electronically controlled engines, the number of sensors, such as manifold pressure, engine RPM, temperature, and other sensors, is usually greater than the number of actuators, such as throttle angle and fuel injection actuators. Consequently, $m \geq p$ and we can construct more than one residual generator (up to C_p^m ones) for actuator failure isolation, so that more information about actuator failures is available. Note that the input signals $u(z)$ and the fault signals in actuators $a(z)$ are indistinguishable. Let Ω denote the set containing all possible combinations in which p sensors can be chosen from m actuators, and let Ω_k denote the k-th subset of Ω. $G_{a,\Omega_k}(z)$ represents the transfer matrix from the actuator inputs to the sensor outputs in Ω_k. $y^{(k)}$ is the output vector of the sensors in Ω_k. For example, to illustrate the above statements a system with 2 inputs and 3 outputs ($p = 2$ and $m = 3$) can be described as follows

$$\begin{aligned} &\Omega = \{\{2,3\},\{1,3\},\{1,2\}\}, \\ &\Omega_1 = \{2,3\},\ \Omega_2 = \{1,3\},\ \Omega_3 = \{1,2\}. \end{aligned} \tag{21}$$

For this case, up to three (C_2^3) residual generators can be constructed for $k = 1, 2$, and 3. After these residual generators are synthesized, their residual output set can be used for multiple-failure detection and isolation. Note that the case of $m = p$ is just a special case of $m \geq p$ in Fig. 2, with the same configuration except that only one pair of $H_a(z)$ and $F_a(z)$ is used.

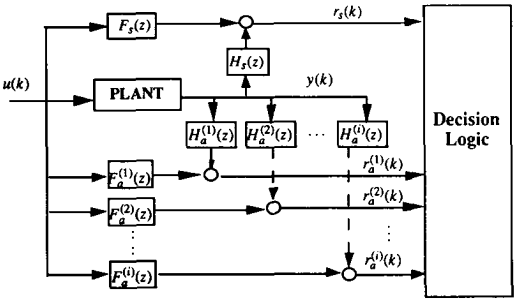

Fig. 2. A general scheme for multiple failure diagnosis.

Also, by choosing $M_a^{(k)}(z)$ for a desirable set of residual generators for actuators, we obtain

$$\begin{aligned} H_a^{(k)}(z) &= M_a^{(k)}(z)G_{a,\Omega_k}^{-1}(z) \\ &\quad \text{(assume } G_{a,\Omega_k}(z) \text{ is invertible)} \end{aligned} \tag{22}$$

and

$$F_a^{(k)}(z) = -M_a^{(k)}(z) \tag{23}$$

for $k = 1, 2, \ldots, C_p^{(m)}(z)$. Then, we have

$$\begin{aligned} r_a^{(k)}(z) &= H_a^{(k)}(z)y^{(k)}(z) + F_a^{(k)}(z)u(z)r_a^{(k)}(z) \\ &= M_a^{(k)}(z)\big(a(z) + G_{a,\Omega_k}^{-1}(z)s^{(k)}(z)\big). \end{aligned} \tag{24}$$

Also, the sensor faults will all affect the output of the residual generators that are designed specifically for actuators. As a result, the designed residual generators will be invalid when simultaneous sensor and actuator failures occur.

As shown in both (20) and (24), failures can be isolated directly by observing r_s and r_a only when actuator and sensor failures do not occur simultaneously. However, if failures occur in both the sensors and actuators, the interaction between faulty sensors and faulty actuators will obscure the direct relationships between failures and residuals in the present scheme. Under such circumstances, a powerful decision logic is required for fault isolation if we are to distinguish different failure conditions.

III. Hexadecimal Decision Table

In this section, we propose a hexadecimal decision table to relate all possible failure patterns of sensors and actuators to residual codes obtained from results of the structured residuals. Here, flags are defined by performing a simple threshold test on residuals as follows:

i) *Threshold test on sensor residuals*

$$\xi_{s_i} = \begin{cases} 1, & \text{if } \|r_{s_i}\| \geq J_{s_i} \\ 0, & \text{if } \|r_{s_i}\| < J_{s_i} \end{cases} \tag{25}$$

ii) *Threshold test on actuator residuals*

$$\xi_{a_i} = \begin{cases} 1, & \text{if } \|r_{a_i}\| \geq J_{a_i} \\ 0, & \text{if } \|r_{a_i}\| < J_{a_i} \end{cases} \tag{26}$$

TABLE I
CAUSE-EFFECT TABLE FOR EXAMPLE 1 ($m = p = 2$)

	a_1	a_2	s_1	s_2
ξ_{s_1}	1	1	1	0
ξ_{s_2}	1	1	0	1
ξ_{a_1}	1	0	1	1
ξ_{a_2}	0	1	1	1

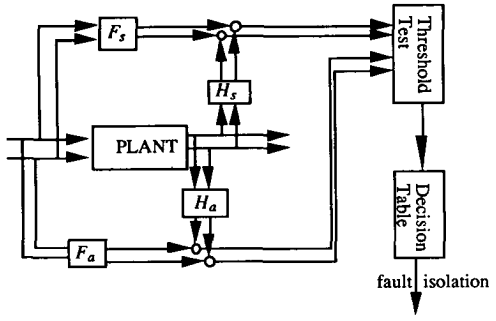

Fig. 3. The general scheme of residual generators for example 1 ($m = p = 2$).

In the general scheme of residual generators, the same test is applied to all residuals to obtain all flags $\xi_{a_i}^{(k)}$ as follows

$$\xi_{a_i}^{(k)} = \begin{cases} 1, & \text{if } \|r_{a_i}^{(k)}\| \geq J_{a_i}^{(k)} \\ 0, & \text{if } \|r_{a_i}^{(k)}\| < J_{a_i}^{(k)} \end{cases} \tag{27}$$

where $\|\cdot\|$ denotes a measure of magnitude (either in the time domain or in the frequency domain) and J_{s_i} and $J_{a_i}^{(k)}$ denote the corresponding threshold values for sensor residuals and actuator residuals, respectively.

These flags are obtained based on the relationships between the residuals and fault sources. Thus, the flags can be combined as a new representation for various failure conditions to form residual codes in hexadecimal digits. Accordingly, we construct a hexadecimal decision table and apply it to decision making. We illustrate our approach by the following two ideal examples:

Example 1 ($m = p = 2$)*:* In this example, the scheme of residual generators is as shown in Fig. 3. When no faults occur in the sensors and actuators, the effects of all residuals on all flags ξ should be insignificant. If a fault occurs and the magnitude of a residual is greater than a certain threshold value, the corresponding flag ξ should be set to 1; otherwise, it should be set to 0. When the corresponding transfer functions $G_u^{-1}(z)$ in (24) are not zero over the frequency range in which the power of the failure signal is concentrated, the relationships between failures and residuals in this 2-input-2-output case can be described as shown in Table I.

For example, the first row $(1, 1, 1, 0)$ means that ξ_{s_1} is influenced by (a_1, a_2, s_1) but is independent of s_2; the first column $(1, 1, 1, 0)^T$ means that the failure of a_1 makes $(\xi_{s_1}, \xi_{s_2}, \xi_{a_1})$ nonzero but has no effect on ξ_{a_2}. Similar interpretations can be applied to the other columns and rows. With a valid cause-effect table, we can list all possible combinations of failure conditions and the corresponding residual patterns. For example, if we use 1's and 0's to denote "fault" and "no fault," respectively, then there are four types of possible failure conditions of the two actuators $\{a_1, a_2\}$: $(00), (01), (10)$, and (11).

TABLE II
HEXADECIMAL DECISION TABLE FOR EXAMPLE 1 ($m = p = 2$)

$(a_1,a_2) \rightarrow$ $\downarrow(s_1,s_2)$	00	01	10	11
00	0	D	E	F
01	7	F	F	F
10	B	F	F	F
11	F	F	F	F

The same argument can be applied to the sensor failure conditions. For example, $(s_1, s_2, a_1, a_2) = (0010)$ represents the condition where actuator a_1 has failed. By putting the residual flags into an ordered pair $(\xi_{s_1}, \xi_{s_2}, \xi_{a_1}, \xi_{a_2})$, we define a residual code in hexadecimal digits to represent each particular pattern of residuals. For instance, if $(\xi_{s_1}, \xi_{s_2}, \xi_{a_1}, \xi_{a_2}) = (1110) =$ "E", it is clear that r_{s_1}, r_{s_2}, and r_{a_1} all exceed their threshold values and the corresponding component a_1 fail. A more concise statement is in the following:

$$(s_1, s_2, a_1, a_2) = (0010) \Leftrightarrow (\xi_{s_1}, \xi_{s_2}, \xi_{a_1}, \xi_{a_2}) = \text{"}E\text{"} = (1110).$$

Additional examples would be these:

$$(s_1, s_2, a_1, a_2) = (0100) \Leftrightarrow (\xi_{s_1}, \xi_{s_2}, \xi_{a_1}, \xi_{a_2}) = \text{"7"} = (0111)$$

$$(s_1, s_2, a_1, a_2) = (1000) \Leftrightarrow (\xi_{s_1}, \xi_{s_2}, \xi_{a_1}, \xi_{a_2}) = \text{"}B\text{"} = (1011).$$

Thus, we can establish a hexadecimal decision table including all possible failure conditions, as shown in Table II. In the hexadecimal decision table, the row elements are the actuator failure conditions and the column elements are the sensor failure conditions.

According to Table II, partial failure conditions, which are located in the upper-left-hand part of the table, can be detected and isolated successfully. If different failure conditions are represented by the same residual code, they cannot be distinguished from one another, as in the lower-right-hand part of the table. For example, the failure conditions with the same residual code "F" in Table II cannot be distinguished from one another, because one of the possible failure conditions may occur as follows:

1) all sensors have failed,
2) all actuators have failed, and
3) any sensor and any actuator have failed at the same time.

In this case, the corresponding failure conditions are not identifiable merely by applying the present hexadecimal decision table. Unless *a priori* knowledge of all failures occurring in the same sector is provided, as in conditions 1) and 2), and the failures can be identified by directly examining the residual outputs. An additional sensor should be employed to extract more information about failures, as illustrated in Example 2.

Example 2 ($m = 3$ and $p = 2$): When an additional sensor is added to the diagnostic system, the overall scheme is as shown in Fig. 4 and the relationships between failures and residuals are as shown in Table III. Similarly, we put the residual flags in ordered pairs as $(\xi_{s_1}, \xi_{s_2}, \xi_{s_3}, \xi_{a_1}^{(3)}, \xi_{a_2}^{(3)}, \xi_{a_1}^{(2)}, \xi_{a_2}^{(2)}, \xi_{a_1}^{(1)}, \xi_{a_2}^{(1)})$. Also, we need to redefine the residual code in

TABLE III
CAUSE-EFFECT TABLE FOR EXAMPLE 2 ($m = 3$, $p = 2$)

	a_1	a_2	s_1	s_2	s_3
ξ_{s_1}	1	1	1	0	0
ξ_{s_2}	1	1	0	1	0
ξ_{s_3}	1	1	0	0	1
$\xi_{a_1}^{(3)}$	1	0	1	1	0
$\xi_{a_2}^{(3)}$	0	1	1	1	0
$\xi_{a_1}^{(2)}$	1	0	1	0	1
$\xi_{a_2}^{(2)}$	0	1	1	0	1
$\xi_{a_1}^{(1)}$	1	0	0	1	1
$\xi_{a_2}^{(1)}$	0	1	0	1	1

TABLE IV
HEXADECIMAL DECISION TABLE FOR EXAMPLE 2 ($m = 3$ and $p = 2$)

$(a_1,a_2) \rightarrow$ $\downarrow(s_1,s_2,s_3)$	00	01	10	11
000	000	1D5	1EA	1FF
001	04F	1DF	1EF	1FF
010	0B3	1F7	1FB	1FF
011	0FF	1FF	1FF	1FF
100	13C	1FD	1FE	1FF
101	17F	1FF	1FF	1FF
110	1BF	1FF	1FF	1FF
111	1FF	1FF	1FF	1FF

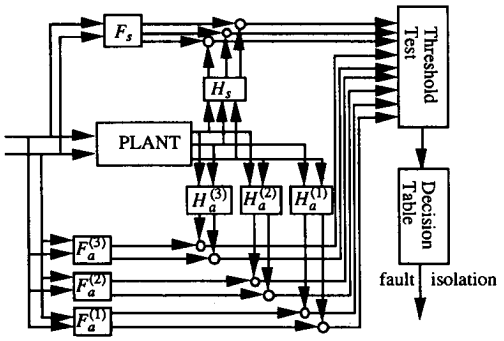

Fig. 4. The general scheme of residual generators for Example 2 ($m = 3$ and $p = 2$).

hexadecimal digits to represent the failure patterns, as shown in Table IV.

In this example, more failure conditions can be identified. For instance, if both sensor s_3 and actuator a_1 have failed at the same time, then the corresponding residual code "1EF" would be expressed as

$$(s_1, s_2, s_3, a_1, a_2) = (00110)$$
$$\Leftrightarrow \left(\xi_{s_1}, \xi_{s_2}, \xi_{s_3}, \xi_{a_1}^{(3)}, \xi_{a_2}^{(3)}, \xi_{a_1}^{(2)}, \xi_{a_2}^{(2)}, \xi_{a_1}^{(1)}, \xi_{a_2}^{(1)}\right)$$
$$= (111101111) = \text{"1EF"}.$$

The percentage of identified failure conditions for the case with one additional sensor is thus increased, as shown by comparing Table IV with Table II. Thus, in this case diagnosis of multiple failures is possible. This result renders useful information about how many extra sensors are required and where to place sensors properly to isolate failure conditions. According to Table IV, only the following failure conditions, all with residual code "1FF," cannot be distinguished from one another:

TABLE V
HEXADECIMAL DECISION TABLE FOR EXAMPLE 2 (THE ADDITIONAL SENSOR IS NORMAL)

$(a_1,a_2) \rightarrow$ $\downarrow(s_1,s_2)$	00	01	10	11
00	000	1D5	1EA	1FF
01	0B3	1F7	1FB	1FF
10	13C	1FD	1FE	1FF
11	1BF	1FF	1FF	1FF

TABLE VI
HEXADECIMAL DECISION TABLE FOR EXAMPLE 2 (THE ADDITIONAL SENSOR IS FAULTY)

$(a_1,a_2) \rightarrow$ $\downarrow(s_1,s_2)$	00	01	10	11
00	04F	1DF	1EF	1FF
01	0FF	1FF	1FF	1FF
10	17F	1FF	1FF	1FF
11	1FF	1FF	1FF	1FF

1) all sensors have failed,
2) all actuators have failed, and
3) two or more sensors have failed at the same time as any actuator has also failed.

Remark: To analyze the improvement in diagnostic performance by adding the extra sensor, we separate Table IV of Example 2 into Table V and Table VI. Table V shows the results when the additional sensor s_3 is operating normally, and Table VI shows the results when s_3 fails. With this additional sensor, the total number of identifiable failure conditions increases from 5 (in Table II) to 10 (in Table V) among 16 possible failure conditions. Even in the worst case, when the additional sensor s_3 also fails, the number of identifiable failure conditions in Table VI is the same as that in Table II. Altogether, the identifiable rate is increased from 5/16 to 15/32 in this ideal case. Normally, to extract more failure information in a diagnostic system additional sensors are maintained in good condition. Therefore, we conclude that for this two-in-two-out system, the percentage of identifiable failures increases from 5/16 to 5/8 if an additional sensor is used. This result justifies the claim that adding a sensor to the system will enhance its performance in isolating simultaneous sensor and actuator failures. However, the number of sensors cannot be increased arbitrarily and we must consider the trade-off between cost and diagnostic performance, and if the sensors are dependent on one another, they may render redundant information. Moreover, because of uncertainty and noise some transfer functions between faults and their residual output may approach zero even when faults occur or may be nonzero even without failure occurrence. The result of the selection of robust threshold is provided in the Appendix.

IV. SIMULATION RESULTS ON ENGINE SENSORS AND ACTUATORS

The diagnostic scheme developed above is applied here to an automotive engine model to illustrate the scheme's on-line fault detection and isolation functions. According to [19], the parameters and the variables of a Corvette 5.7 liter multi-port

fuel injected engine with a GMP4 engine controller are as follows:

$$A = \begin{bmatrix} 0.779 & 0.0632 & -0.149 & -0.635 & -0.211 \\ 1 & 0 & 0 & 0 & 0 \\ 0.271 & -0.253 & 0.999 & 0 & 0.845 \\ 0 & 0 & 0 & 0 & 0 \\ 0 & 0 & 0 & 0 & 0 \end{bmatrix}, \tag{28}$$

$$B = \begin{bmatrix} 1.5796 & 0.22598 \\ 0 & 0 \\ 0 & -0.9054 \\ 1 & 0 \\ 0 & 1 \end{bmatrix}, \tag{29}$$

and

$$C = \begin{bmatrix} 1 & 0 & 0 & 0 & 0 \\ 0 & 0 & 1 & 0 & 0 \end{bmatrix} \tag{30}$$

with two inputs

$u_1(k)$: throttle angle change,
$u_2(k)$: change in external load,

and two outputs

$y_1(k)$: change in manifold pressure, and
$y_2(k)$: change in engine RPM.

Also, there are five states in this engine model:

$x_1(k)$: change in manifold pressure,
$x_2(k)$: $= x_1(k-1)$,
$x_3(k)$: change in engine RPM,
$x_4(k)$: change in throttle position, and
$x_5(k)$: change in external load.

The operating conditions are as follows:

engine speed:	1730 rpm,
manifold pressure:	14.4 in-Hg,
throttle angle position:	17.9% max. opening,
external load torque:	56.3 Ft-Lb.

For in-house diagnosis, all measurements including the external load torque are assumed to be measurable and artificial faults are provided in the simulation. If *a priori* knowledge of all failures that occur in the same sector is available, the residual outputs of the present scheme explicitly indicate all the failure sources, as discussed in Case 1 and Case 2.

Case 1 Multiple Sensor Failures: When all failures occur in the sensors, the general scheme of residual generators generates decoupled residual signals corresponding to each sensor fault. Assume that sensor s_2 fails at $k = 20$ with a bias of -2 and sensor s_1 fails at $k = 40$ with a bias of $+1$. In this case, we obtain the residual output signals, as shown in Fig. 5, simply by using a unit matrix as the residual map. Clearly, the signals exhibit the same information as the true failure conditions and thus all sensor failures can be isolated by examining the residuals directly.

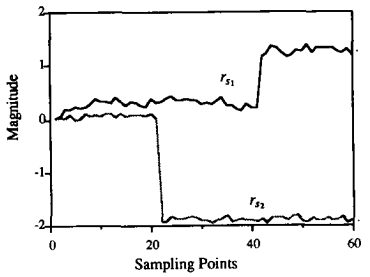

Fig. 5. Sensor residual signals (Case 1).

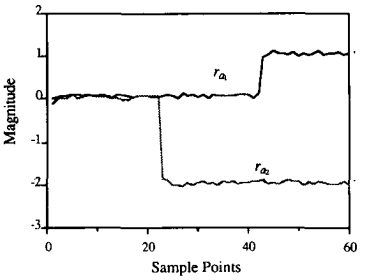

Fig. 6. Actuator residual signals (Case 2).

Case 2 Multiple Actuator Failures: Similarly, decoupled residuals for multiple actuator failures can be obtained when all failures occur in the actuators. For simulation, we assume that even the actuator a_2 of the external load will fail in the in-house diagnosis at $k = 20$ with a bias of -2 and actuator a_1 of the throttle angle fails at $k = 40$ with a bias of $+1$. Since the propagation of faults from actuators to residuals through the engine system causes the time lag, we design the residual generators for the actuator with poles all at 0.1, and the residual output signals are obtained as shown in Fig. 6. Also, the residuals exhibit the same information as the true failure conditions. Therefore, all multiple actuator faults can again be isolated by examining the residuals directly.

In the following two cases, multiple faults occur in both sensors and actuators simultaneously, further decision logic is required, and we apply the proposed hexadecimal decision table.

Case 3 Multiple Sensor and Actuator Failures ($m = p = 2$)*:* In this case, we adopt the same residual maps as in the above two cases for sensors and actuators separately. When actuator a_1 fails at $k = 20$ with a bias of $+1$ and sensor s_2 fails at $k = 40$ with a bias of -1, the residual outputs as shown in Fig. 7(a)–(b) which are affected by both failures cannot be directly used to isolate the fault sources. Therefore, the cause-effect table and hexadecimal decision table presented in Tables I and II are then used. When the proposed decision technique is applied, the residual code in the diagnostic procedure changes from "0" to "E" when $k > 20$ and from "E" to "F" after $k > 40$, as shown in Fig. 7(c). These diagnostic results are justified by the true failure conditions. However, when simultaneous failures occur in this case, the code "F" cannot identify the exact failure pattern. Therefore, the diagnosis performance must be improved by implementing another sensor to acquire more failure information, as discussed in the next case.

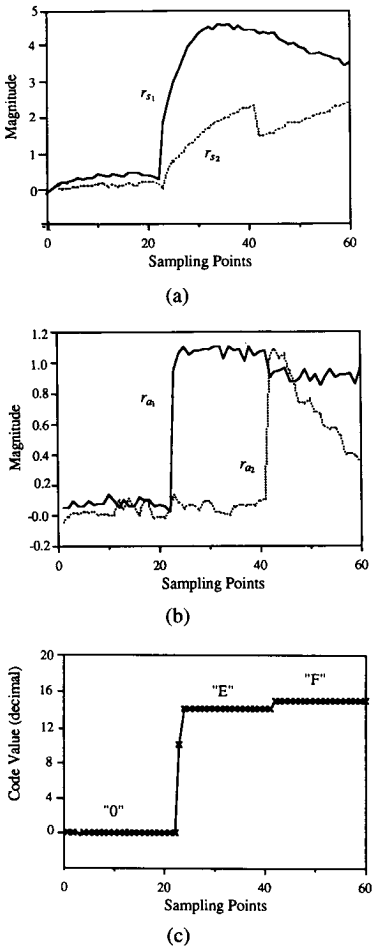

Fig. 7. (a) Sensor residual signals, (b) actuator residual signals, and (c) residual code plot for Case 3 ("0": no fault; "E": a_1 fault; "F": unidentified fault).

Case 4 Multiple Sensor and Actuator Failures ($m = 3$ and $p = 2$): If an additional throttle angle sensor is available [20], the system parameter C in (30) can be augmented as follows:

$$C = \begin{bmatrix} 1 & 0 & 0 & 0 & 0 \\ 0 & 0 & 1 & 0 & 0 \\ 0 & 0 & 0 & 1 & 0 \end{bmatrix}. \tag{31}$$

We then redesign the residual generators with the same dynamics as in the above cases. Due to some zero transfer metrics between the faults and residuals, we reconstruct the cause-effect table and a hexadecimal decision table as shown in Tables VII and VIII. Consider the same failure conditions as in Case 3, where the residual code changes from "000" to "1EA" when $k > 20$ and from "1EA" to "1FB" after $k > 40$, as shown in Fig. 8. Clearly, multiple failures are isolated properly according to their true failure conditions. Also note that the results of this case are slightly different from those of the ideal case discussed in Example 2, with reference to Tables III and IV. Two sets of failure conditions, with residual codes "1B5" and "1FF," cannot be distinguished exactly in Table VIII, because three sets of residuals that are nearly zero appear in Table VII even when failures occur. As a result, their failure conditions are difficult to identify under noise contamination.

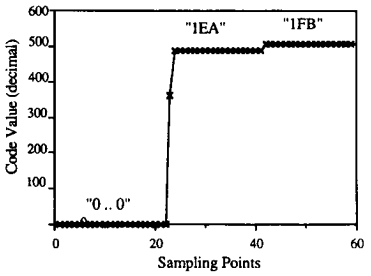

Fig. 8. Residual code plot (Case 4) ("000": No fault; "1EA": a_1 fault; "1FB": a_1 and s_2 faults).

TABLE VII
CAUSE-EFFECT TABLE FOR CASE 4

	a_1	a_2	s_1	s_2	s_3
ξ_{s1}	1	1	1	0	0
ξ_{s2}	1	1	0	1	0
ξ_{s3}	1	0	0	0	1
$\xi^{(3)}_{a1}$	1	0	1	1	0
$\xi^{(3)}_{a2}$	0	1	1	1	0
$\xi^{(2)}_{a1}$	1	0	0	0	1
$\xi^{(2)}_{a2}$	0	1	1	0	1
$\xi^{(1)}_{a1}$	1	0	0	0	1
$\xi^{(1)}_{a2}$	0	1	0	1	1

TABLE VIII
HEXADECIMAL DECISION TABLE FOR CASE 4

$(a_1,a_2) \rightarrow$ $\downarrow(s_1,s_2,s_3)$	00	01	10	11
000	000	195	1EA	1FF
001	04F	1DF	1EF	1FF
010	0B1	1B5	1FB	1FF
011	0FF	1FF	1FF	1FF
100	134	1B5	1FE	1FF
101	17F	1FF	1FF	1FF
110	1B5	1B5	1FF	1FF
111	1FF	1FF	1FF	1FF

V. EXPERIMENTAL RESULTS

In this section, the results of the test cell experiments, which took place at the Engine Development Department, Industrial Technology Research Institute, Taiwan, are presented. A Nissan GA16DE 1597 c.c. engine with its ECCS electronic control unit was used. The engine was implemented on a Midwest Eddy current dynamometer with the Schenk control unit. Theoretically, the analytical model of engine systems is [19]

$$\Delta \dot{P}_M(t) = k_1 \Delta\theta(t) - k_2 \Delta P_M(t) - k_3 \Delta N(t), \tag{32}$$

$$\Delta T_I(t) = k_4 \Delta P_M(t - t_D), \tag{33}$$

and

$$\Delta \dot{N}(t) = \frac{1}{J}(\Delta T_I(t) - \Delta T_L(t) - k\Delta N(t)). \tag{34}$$

where the "Δ" represents the deviation from the operation point, and $N(k)$ and $P_M(k)$ indicate the engine speed and manifold pressure, respectively. θ, T_I, and T_L are the throttle angle opening, the indicated torque, and the external load torque, respectively. The inertia of the engine is denoted by

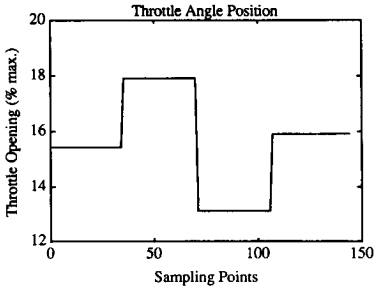

(a)

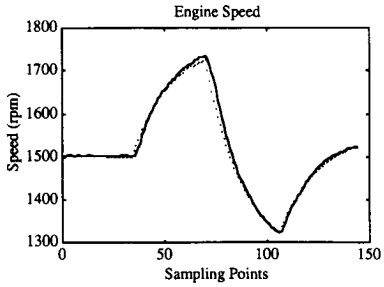

(b)

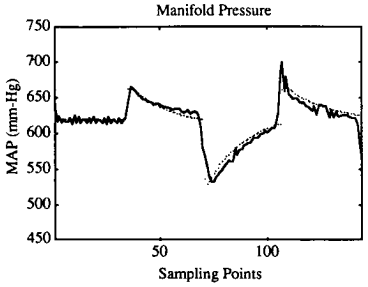

(c)

Fig. 9. Experimental results (solid) and simulation results (dotted) of model verification. (a) Throttle angle position, (b) engine speed, (c) manifold pressure.

"J". For this diagnostic experimental setup, we neglect the transmission delay t_D and include the indicated torque T_I in the term of the load torque T_L. Hence here the engine model of (32)–(34) is expressed as

$$\Delta N(k+1) = k_1 \Delta N(k) + k_2 \Delta\theta(k) + k_3 \Delta T_L(k) \quad (35)$$

$$\Delta P_M(k+1) = k_4 \Delta P_M(k) + k_5 \Delta N(k) + k_6 \Delta\theta(k). \quad (36)$$

The tested operating conditions where the sampling period 0.04 s were as follows

engine speed	1500 rpm,
manifold pressure	620 mm-Hg,
throttle angle position	15.4% max. opening, and
external load torque	64.5 Nt-m.

By varying the $\Delta\theta$ and ΔT_L with both speed and torque control modes, the parameters of this engine model can be obtained from experimental results as follows:

$$\begin{bmatrix} \Delta P_M(k+1) \\ \Delta N(k+1) \end{bmatrix} = \begin{bmatrix} 0.1485 & -0.1940 \\ 0 & 0.9440 \end{bmatrix} \begin{bmatrix} \Delta P_M(k) \\ \Delta N(k) \end{bmatrix} + \begin{bmatrix} 17.1950 & -0.1103 \\ 5.8000 & -3.2479 \end{bmatrix} \begin{bmatrix} \Delta\theta(k) \\ \Delta T_L(k) \end{bmatrix}. \quad (37)$$

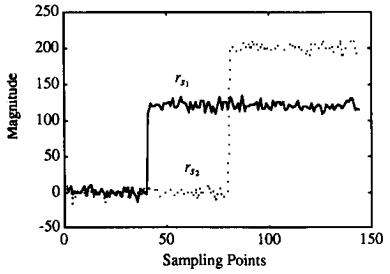

Fig. 10. Sensor residual signals (Case 5).

TABLE IX
HEXADECIMAL DECISION TABLE FOR CASE 6 ($m = p = 2$)

$(a_1,a_2) \rightarrow$ / $\downarrow(s_1,s_2)$	00	01	10	11
00	0	D	E	F
01	6	F	E	F
10	B	F	F	F
11	F	F	F	F

When the external load was maintained as constant and the throttle angle position varied as shown in Fig. 9(a), the simulation responses of MAP and speed, as shown in Figs. 9(b) and (c), respectively, were in good agreement with the experimental results. Therefore, the present linearized model is adequate for diagnostic design when the engine is operated around the predetermined conditions. Experimental results on engine diagnosis of multiple actuator and sensor failures are discussed as below.

Case 5 Multiple Sensor Failures: Similar to Case 1, when artificial failures of a bias of 120 (mm-Hg) for the MAP sensor s_1 at $k = 40$ and a bias of $+200$ (rpm) for the speed sensor s_2 at $k = 80$ were caused. The residual output signals are shown in Fig. 10. The signals exhibit information similar to the true failure conditions, although negligible peaks of a short duration appear in the residuals, mainly because of modeling error. In this case, all sensor failures can be isolated by examining the residuals directly.

Case 6 Multiple Sensor and Actuator Failures ($m = p = 2$): Faults were invoked for the actuator of the throttle angle a_1 at $k = 40$ with a bias of 10 (% max. opening) and for the MAP sensor s_1 at $k = 80$ with a bias of 120 (mm-Hg). As shown in Fig. 11(a) and (b), the residual output due to the simultaneous faults cannot be used directly to isolate the fault sources. Further decision making via the hexadecimal decision table is thus required. In this case we construct the hexadecimal decision table as shown in Table IX. As shown in Fig. 11(c), the residual code in the on-line diagnosis changes from "0" to "E" when $k > 40$ and from "E" to "F" after $k > 80$. According to Table IX, the fault in this case can be identified only when a single failure occurs, and none of the multiple failure conditions denoted by "F" can be isolated. Therefore, further diagnosis should be conducted by implementing an additional sensor to extract more failure information, as discussed in the next case.

Case 7 Multiple Sensor and Actuator Failures ($m = 3$ and $p = 2$): In this case, one additional sensor is added to measure throttle angle. We can construct another hexadecimal decision table, as shown in Table X. With the same fault conditions

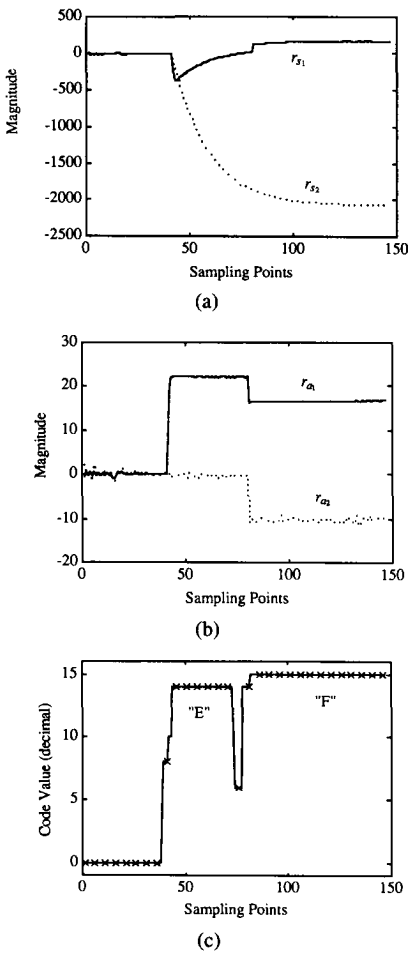

Fig. 11. (a) Sensor residual signals, (b) actuator residual signals, and (c) residual code plot (Case 6).

as in Case 6, the residual code in the diagnostic procedures changes from "000" to "1EA" when $k > 40$ and from "1EA" to "1FE" after $k > 80$, as shown in Fig. 12. Under the assumption that the additional sensor is functioning normally, the present identified fault conditions indeed correspond to the true multiple failure conditions. Compared with the simulation results in Example 2, the experimental results indicate that diagnostic system identifies fewer failure patterns in real applications than in ideal cases, because some cause-effect elements are either nearly zero or are contaminated by noise and system uncertainty even without failure occurrence.

VI. Limitations and Improvements

The simulation and experimental results presented above confirm the applicability of the present approach to diagnosing sensor and actuator failures. However, in real applications, the present approach has unavoidable limitations and possible improvements to the present approach are discussed below.

1) The present approach is based on a linearized model of an automotive engine as shown in (37). Although experimental results on model verification have proven the validity of the present model, the operating conditions of the engine system must be close to the predetermined conditions for the model to remain valid. Moreover, noise contamination and system uncertainty, as well as the zero transfer matrices in some modes of the system, degrade the performance of the present diagnostic design seriously, as shown in the experimental results. Therefore, robust residual dynamics and thresholds must be specified in the real diagnostic design.
2) The present approach is suitable for in-house engine diagnosis with all measurements of model variables. However, the external load torque is not a real actuator and is unmeasurable in real applications. Therefore, a special form of residual generators, an unknown input fault detection observer (UIFDO) that decouples the external load from the residual outputs, is needed for on-road diagnosis [21]. When a car is either idling or cruising, the external load maintains a constant value. Under such circumstances, the loading torque can be predicted so that the present approach is still valid for on-road testing.
3) Since the cause-effect table is constructed without redundancy, as shown in Tables I and III, simplification of the present scheme can be achieved only if partial failure patterns are identified. On the other hand, an additional sensor is required to improve the identifiable failure rate, especially in the case of simultaneous sensor and actuator failures. In practice, the improvement obtained by implementing more sensors is limited, because extra sensors may render redundant information and some physical variables are difficult to measure directly.
4) Basically, the present residual generators are effective in cases of additive faults. To identify multiplicative faults and to evaluate their exact size, system parameter estimation is a more appropriate method [22]. Furthermore, diagnosis of engine components is also important. Therefore, for the overall engine diagnosis, it is crucial

TABLE X
Hexadecimal Decision Table For Case 7 ($m = 3$ and $p = 2$)

$(a_1,a_2) \rightarrow$ / $\downarrow(s_1,s_2,s_3)$	00	01	10	11
000	000	195	1EA	1FF
001	04B	1DF	1EB	1FF
010	0A1	1B5	1EB	1FF
011	0EB	1FF	1EB	1FF
100	134	1B5	1FE	1FF
101	17F	1FF	1FF	1FF
110	1B5	1B5	1FF	1FF
111	1FF	1FF	1FF	1FF

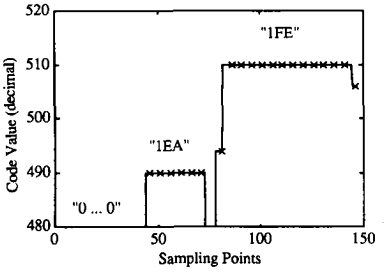

Fig. 12. Residual code plot (Case 7).

to develop more effective approaches that incorporate both the state and parameter estimation methods.

VII. Conclusion

This paper introduces a diagnostic system to achieve detection and isolation of multiple sensor and actuator failures in automotive engines. We have proposed a general scheme of residual generators to construct a hexadecimal decision table for identifying all possible failure patterns in residual codes. Both simulation and experimental results indicate that the proposed diagnostic system not only can be applied to cases where all failures occur in the same sector, but is also appropriate for isolating multiple failures occurring simultaneously in sensors and actuators. Diagnostic results on automotive engine sensors and actuators verify the feasibility of the proposed approach.

Appendix

To determine robust threshold, it is assumed that the modeling error is in the multiplicative form as

$$\tilde{G}_u = (I + \Delta)G_u.$$

Moreover, assume that the modeling error, actuator noise w, and sensor noise n are bounded and the upper bound of each is known, as follows:

$$\bar{\sigma}(\Delta(j\omega)) \le \delta(\omega), \qquad ||w(j\omega)||_2 \le \bar{w},$$

and

$$||n(j\omega)||_2 \le \bar{n}.$$

When the system is free from any fault, the J_{miss} can be defined as the maximal possible norm for residual signal r. A fault occurrence is declared only when the residuals is larger than the threshold value J_{th} as

$$J_{\text{miss}} = \sup_{R,w,n,\Delta} ||r||$$
$$J_{\text{th}} > J_{\text{miss}}.$$

A necessary and sufficient condition for declaring an alarm is when the norm of the residue r surpasses the threshold J_{th} as follows:

$$\inf_{R,w,n,\Delta} ||r|| > J_{\text{th}}.$$

By defining an innovation sequence $e(s)$ as

$$\begin{aligned} e(s) &= \Delta(I + \Delta T)^{-1}TR(s) + (I + \Delta T)^{-1}(I + \Delta)G_u w(s) \\ &\quad + (I + \Delta T)^{-1}n(s) \\ &= T_{eR}(s)R(s) + T_{ew}(s)w(s) + T_{en}(s)n(s) \end{aligned} \tag{A-1}$$

where

$$T(s) := (I + G_u(s)K(s))^{-1}G_u(s)K(s) \tag{A-2}$$

and $K(s)$ is the controller. Then, we have

$$r(s) = H(s)e(s) =: \begin{bmatrix} H_1(s) \\ \vdots \\ H_q(s) \end{bmatrix} e(s), \tag{A-3}$$

that

$$r_i(s) = H_i(s)e(s), \qquad \text{for } i = 1, 2, \ldots, q. \tag{A-4}$$

Consequently, we can determine the robust fault isolation threshold $J_{\text{th}i}$ for the i-th residual as follows [17]:

$$\begin{aligned} J_{\text{miss}i} &= \sup_{R,w,n,\Delta} |r_i(t)| \\ &= \sup_{R,w,n,\Delta} |H_i(t) * e(t)| \\ &\le \sup_{R,w,n,\Delta} ||H_i(t)||_2 \, ||e||_2 \\ &= \sup_{R,w,n,\Delta} ||H_i||_2 \, ||T_{eR}R + T_{ew}w + T_{en}n||_2 \\ &\le ||H_i||_2 \cdot \Big\{ ||R(j\omega)||_2 \cdot \sup_{\Delta} ||T_{eR}||_\infty \\ &\qquad + \bar{w} \cdot \sup_{\Delta} ||T_{ew}||_\infty + \bar{n} \cdot \sup_{\Delta} ||T_{rn}||_\infty \Big\} \\ &\le ||H_i||_2 \cdot \Big\{ ||R(j\omega)||_2 \\ &\qquad \cdot \sup_{\omega \in R} \left[\frac{\delta(\omega) \cdot \bar{\sigma}(T(j\omega))}{1 - \delta(\omega) \cdot \bar{\sigma}(T(j\omega))} \right] \\ &\qquad + \bar{w} \cdot \sup_{\omega \in R} \left[\frac{(1 + \delta(\omega)) \cdot \bar{\sigma}(G_u(j\omega))}{1 - \delta(\omega) \cdot \bar{\sigma}(T(j\omega))} \right] \\ &\qquad + \bar{n} \cdot \sup_{\omega \in R} \left[\frac{1}{1 - \delta(\omega) \cdot \bar{\sigma}(T(j\omega))} \right] \Big\} \\ &= J_{\text{th}i}. \end{aligned} \tag{A-5}$$

To make the problem more tractable, we can further adopt the simplifying assumption that the reference input is a step $R(t) = \bar{R}1(t)$ and the bound on model error $\Delta(s)$ is constant $\bar{\eta}$, and $\Delta(s)$ is sufficiently small so that

$$(I + \Delta(s)T(s))^{-1} \approx I.$$

Then the threshold can be approximated as

$$J_{\text{th}i} \approx ||H_i||_2 \times \{\bar{R} \cdot \bar{\eta} \cdot ||T||_\infty + \bar{w} \cdot (1 + \bar{\eta}) \cdot ||G_u||_\infty + \bar{n}\}. \tag{A-6}$$

Acknowledgment

The authors would like to thank the editor and reviewers for their helpful comments on the paper. Also, the authors are grateful to Mr. J. H. Wang, Mr. Y. C. Lin, Dr. S. S. Lin and Mr. M. H. Jeng of the Engine Development Department, Industrial Technology Research Institute, Taiwan, for their assistance in conducting the engine tests.

References

[1] R. J. Patton, P. M. Frank, and R. N. Clark, *Fault diagnosis in dynamic systems: Theory and applications*. Englewood Cliffs, NJ: Prentice-Hall, 1989.

[2] A. S. Willsky, "A survey of design methods for failure detection in dynamic systems," *Automatica*, vol. 12, no. 6, pp. 601–611, 1976.

[3] R. Isermann, "Process fault detection based on modeling and estimation methods—A survey," *Automatica*, vol. 20, no. 4, pp. 387–404, 1984.

[4] P. M. Frank, "Fault diagnosis in dynamic systems using analytical and knowledge-based redundancy—A survey and some new results," *Automatica*, vol. 26, no. 3, pp. 459–474, 1990.

[5] J. Gertler, "Residual generation in model-based fault diagnosis," *Control-Theory Advanced Technol.*, vol. 9, no. 1, pp. 259–285, 1993.

[6] G. Rizzoni and P. S. Min, "Detection of sensor failures in automotive engines," *IEEE Trans. Veh. Technol.*, vol. 40, no. 2, pp. 487–500, May 1991.
[7] P. S. Min and W. B. Ribbens, "A vector space solution to incipient sensor failure detection with applications to automotive environments," *IEEE Trans. Veh. Technol.*, vol. 38, no. 3, pp. 148–158, 1989.
[8] C. D. de Benito, "On-board real time failure detection and diagnosis of automotive systems," *Proc. American Contr. Conf.*, June 1988, pp. 2401–2405.
[9] R. N. Montgomery and A. K. Caglayan, "Failure accommodation in digital flight control systems by Bayesian decision theory," *J. Aircraft*, vol. 13, pp. 69–75, 1976.
[10] A. S. Willsky, J. J. Jr. Deyst, and B. S. Crawford, "Adaptive filtering and self-test methods for failure detection and compensation," *Proc. 1974 Automatic Control Conf.*, 1974, pp. 637–645.
[11] R. N. Clark and W. Setzer, "Sensor fault detection in a system with random disturbances," *IEEE Trans. Aerosp. Electron. Syst.*, vol. AES-16, no. 4, pp. 468–473, 1980.
[12] R. N. Clark, "A simplified instrument failure detection scheme," *IEEE Trans. Aerosp. Electron. Syst.*, vol. AES-14, no. 3, pp. 558–563, 1978.
[13] P. M. Frank and L. Keller, "Sensitivity discriminating observer design for instrument fault detection," *IEEE Trans. Aerosp. Electron. Syst.*, vol. AES-16, no. 4, pp. 460–467, 1980.
[14] X. Ding and P. M. Frank, "Fault detection via factorization approach," *System & Control Letters*, vol. 14, no. 5, pp. 431–436, 1990.
[15] M.-A. Massoumnia and W. E. V. Velde, "Generating parity relations for detecting and identifying control system component failures," *AIAA J. Guidance Cont. Dynamics*, vol. 11, no. 1, pp. 60–65, 1988.
[16] M.-A. Massoumnia, G. C. Verghese, and A. S. Willsky, "Failure detection and identification," *IEEE Trans. Automat. Contr.*, vol. 34, no. 3, pp. 316–321, 1989.
[17] S. K. Chang and P. L. Hsu, "A parametric transfer matrix approach to fault identification filter design and threshold selection," *Int. J. Syst. Sci.*, to be published.
[18] N. Viswanadham, J. H. Taylor, and E. C. Luce, "A frequency-domain approach to failure detection and isolation with application to GE-21 turbine engine control systems," *Cont. Theory Adv. Technol.*, vol. 3, no. 1, pp. 45–72, 1987.
[19] P. S. Min, "Diagnosis of on-board sensors in internal combustion engines," *Proc. American Contr. Conf.*, 1989, pp. 1065–1070.
[20] ——, "Validation of controller inputs in electronically controlled engines," *Proc. American Contr. Conf.*, 1990, pp. 2887–2890.
[21] S. K. Chang and P. L. Hsu, "Fault detection observer design for linear systems with unknown inputs," *2nd ECC*, Groningen, The Netherlands, June 1993, pp. 1975–1980.
[22] R. Isermann, "Fault diagnosis of machines via parameter estimation and knowledge processing—Tutorial Paper," *Automatica*, vol. 29, no. 4, pp. 815–835, 1993.

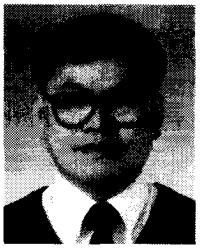

Pau-Lo Hsu (M'92) received the B.S. degree from National Cheng Kung University, Taiwan, R.O.C., the M.S. degree from the University of Delaware, and the Ph.D. degree from the University of Wisconsin-Madison, in 1978, 1984 and 1987, respectively, all in mechanical engineering.

He worked as a manufacturing engineer at the San-Yang (Honda) Industry, Taiwan, after he finished his bachelor degree. He then worked as a sales engineer with the specialty in cutting tools at the Sandvik Taiwan Ltd. After he finished his graduate studies, he worked as a research associate at the Department of Neurophysiology, University of Wisconsin-Madison. In 1988, he joined the Department of Control Engineering, National Chiao Tung University, Taiwan, R.O.C., where he is currently an Associate Professor. His research interests include CNC machining processes, motion control, and fault diagnostic systems.

Ken-Li Lin received the B.S. and M.S. degrees from the National Chiao Tung University, Taiwan, R.O.C., in 1990 and 1992, respectively, both in control engineering.

He is now a system engineer at AT&T Taiwan Telecommunications Co., Ltd.

Li-Cheng Shen received the B.S. and M.S. degrees from the National Chiao Tung University, Taiwan, R.O.C., in 1992 and 1994, respectively, both in control engineering. He is currently a Ph.D. candidate in the Institute of Electronic Engineering at the National Chiao Tung University.

His research interests include the theory and applications of diagnostic systems.